Elsevier Editorial System(tm) for Computers and Structures
Manuscript Draft

Manuscript Number:

Title: Numerical study of confinement effectiveness in solid and hollow reinforced concrete bridge piers : Methodology

Article Type: Research Paper

Section/Category:

Keywords: Confinement; reinforced concrete; bridge piers; hollow sections; finite elements; modelling

Corresponding Author: Dr. Vassilis K. Papanikolaou, Dipl. Eng., MSc DIC, PhD

Corresponding Author's Institution: Aristotle University of Thessaloniki

First Author: Vassilis K. Papanikolaou, Dipl. Eng., MSc DIC, PhD

Order of Authors: Vassilis K. Papanikolaou, Dipl. Eng., MSc DIC, PhD; Andreas J Kappos, Professor

Manuscript Region of Origin:

Abstract: A consistent methodology is suggested for modelling confinement in both solid and hollow reinforced concrete bridge pier sections, using three-dimensional nonlinear finite element analysis. The ultimate goal is to suggest the most convenient transverse reinforcement arrangements in terms of enhanced strength and ductility, as well as ease of construction and cost-effectiveness. Constitutive laws, modelling techniques and preliminary applications are first introduced, followed by a large parametric model setup for circular and rectangular bridge piers of solid and hollow section. A detailed discussion follows on various issues concerning confinement modelling, aiming to broaden the scope and applicability of the suggested methodology.

Numerical study of confinement effectiveness in solid and hollow reinforced concrete bridge piers : Methodology

Vassilis K. Papanikolaou, Andreas J. Kappos

Laboratory of Reinforced Concrete and Masonry Structures, Civil Engineering Department, Aristotle University of Thessaloniki, P.O. Box 482, Thessaloniki, 54124, Greece

Abstract

A consistent methodology is suggested for modelling confinement in both solid and hollow reinforced concrete bridge pier sections, within the computational framework of three-dimensional nonlinear finite element analysis. The ultimate goal is to suggest the most convenient transverse reinforcement arrangements in terms of enhanced strength and ductility, as well as ease of construction and cost-effectiveness. The present study is particularly relevant with respect to confinement of hollow sections, for which previous experimental and analytical research is limited. Constitutive laws, modelling techniques, post-processing issues and preliminary applications are first introduced, and a large parametric model setup for circular and rectangular bridge piers of solid and hollow section, is subsequently presented. A detailed discussion follows on various issues concerning confinement modelling, aiming to broaden the scope and applicability of the suggested methodology. The respective numerical results and their interpretation and evaluation will be presented in a companion paper.

Keywords : Confinement; reinforced concrete; bridge piers; hollow sections; finite elements; modelling

1. Introduction

Efficient seismic design and detailing of bridge piers and pylons requires adequate section deformation capacity (ductility) without significant loss of strength inside the critical regions, especially in the case of monolithic construction, where piers should transfer not only gravity, but also lateral (seismic), forces from the superstructure to the foundations. In order to satisfy these demands, various configurations of section shapes, reinforcement arrangements, and material properties can be employed, usually following code prescriptions and design recommendations (e.g. [1, 2, 3]). Amongst available solutions, hollow pier sections have become increasingly popular in bridge construction during the last decades, especially in Europe [4], featuring considerably reduced concrete mass and hence inertia (seismic) actions. Figure 1 shows a typical configuration of section geometry and transverse (hoop) reinforcement arrangement in circular and rectangular hollow bridge piers.

A key feature that positively contributes to the strength and ductility enhancement of a pier section is the resulting confinement effectiveness. It is well known that the passive confinement mechanism is based on the activation (development of tensile stress) of the transverse reinforcement, which restrains the physical lateral expansion of concrete (Poisson's effect), induced by compressive loading. The ensuing triaxial stress state in the confined material finally leads to a significant increase in the overall strength and deformation capacity of the structural element itself [5].

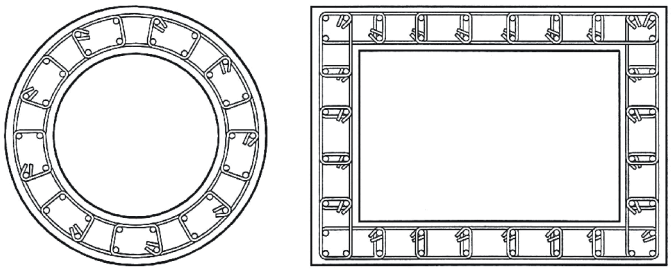

Figure 1. Typical circular (left) and rectangular (right) hollow bridge pier sections [3].

Previous experimental studies mainly conducted during the 80s (e.g. [6, 7] for normal concrete, and [8, 9] for high strength concrete) have clarified most of the

parameters that favourably or adversely affect the effectiveness of passive confinement. The common ground of these studies was the experimental testing of rectangular and circular solid columns confined with various lateral reinforcement arrangements under concentric compressive loading. As a result, various empirical confinement models were proposed, directly based on the above experimental data (e.g. [10, 11, 12]). These models usually provide empirical 'confinement effectiveness' factors, based on the aforementioned experimental parameters (section geometry, transverse reinforcement volumetric ratio, strength, and arrangement, to name a few), which upscale the uniaxial response of plain concrete in terms of strength and ductility, accounting for the presence of confinement reinforcement.

However, to the best of the authors' knowledge, the above analytical models are limited to solid reinforced concrete sections (upon which they were originally calibrated) and their extension to the assessment of hollow pier sections is not straightforward. This is due to the non-standard geometric characteristics of hollow sections, and specifically due to the presence of an inner void, which drastically reduces the effectively confined region. As a result, 'negative confinement' effects may arise, leading to early cracking of the inner concrete cover (implosion) and hence to a reduction of section ductility [13]. As far as the previous experimental work on hollow sections is concerned (e.g. [14, 15, 16, 17]), it is mainly focused on their flexural and shear behaviour under lateral cyclic (seismic) excitation. This is justified by the fact that research on the seismic behaviour of hollow piers is of critical importance to bridge design in earthquake-prone areas (like southern Europe), nonetheless studying the issue of confinement requires pure concentric compressive action in order to (a) drive the specimen beyond its ultimate strength, (b) record the complete capacity curve (axial load vs. axial deformation) including softening and (c) derive the strength and ductility enhancement due to confinement. However, this process is prohibited for full-scaled piers due to the huge mechanical means required, and becomes feasible only for small-scale specimens. In this respect, the available literature is limited to the experimental work by Taylor et al. [18], which included thin-walled hollow sections under low eccentric compression (almost concentric), though without any reference to confinement effectiveness but only to the effect of section thickness on local buckling phenomena. More relevant was the experimental study by Mo et al. [19], including, inter alia, a

parametric study on the confinement effectiveness of different lateral reinforcement anchorage types, hoop spacing and material strengths in hollow sections. The specimens were constructed as single vertical panels (one quarter of a hollow section) without concrete cover, and were axially compressed up to failure. The failure patterns showed mainly concrete crushing and a few longitudinal steel buckling cases for large hoop spacing. There was observed negligible difference between different anchorage types, stronger response for smaller spacing and smaller ductility for high-strength concrete, which are deemed reasonable.

A recent analytical alternative to the empirical uniaxial models for studying the confinement effectiveness of reinforced concrete sections is the direct application of three-dimensional nonlinear finite element analysis. Although this numerical method is demanding on computational resources, its application cost is way reduced compared to its experimental counterpart. Another important advantage is that there are almost no modelling restrictions regarding section geometry and the complexity of transverse reinforcement arrangement. It should be also pointed out that finite element analysis can describe the confinement effect on its fundamental basis, without empirical modifications to material constitutive laws for properly capturing the expected strength and ductility enhancement. The latter remains a drawback for empirical models, which are often limited to the specific experimental setups employed for their calibration [20]. In the last two decades, the boost of available computational power led to a significant number of numerical studies on three-dimensional nonlinear finite element modelling of vertical reinforced concrete elements, featuring various constitutive models, modelling techniques, loading types and confinement arrangements (Tab. 1). However, the available literature is still limited to solid sections, with the exception of the work by Faria et al. [21], where hollow cross-sections are modelled in plane as equivalent I-sections.

In this paper, the main goal is to suggest a consistent methodology for modelling both solid and hollow reinforced concrete bridge pier sections (and generally vertical members) with various transverse reinforcement arrangements, using a general-purpose finite element software, properly enhanced in terms of the concrete constitutive law. The ultimate objective of the present research is to suggest the most convenient confinement arrangements in terms of enhanced strength and ductility, as well as ease of

construction and cost effectiveness. Constitutive laws, modelling techniques, post-processing issues and preliminary applications are covered in the subsequent section. The next section presents a large parametric model setup, including circular and rectangular bridge piers of solid and hollow section, which were based on actually constructed bridges. This is followed by a detailed discussion on various issues concerning confinement modelling, aiming to broaden the scope and applicability of the suggested methodology. The respective numerical results and their interpretation and evaluation will be presented in a companion paper.

Table 1. Previous studies on three-dimensional nonlinear finite element analysis of confined reinforced concrete vertical members

Authors	Structural element type	Concrete law	Reinforcement modelling	Loading type	Confinement type
Abdel-Halim and Abu-Lebdeh [22]	Solid rectangular columns	Nonlinear elasticity	Discrete	Concentric compressive	Transverse reinforcement
Barzegar and Maddipudi [23]	Solid rectangular columns	Nonlinear elasticity	Embedded	Concentric compressive	Transverse reinforcement
Foster et al. [24]	Solid circular columns	Microplane	Discrete axisymmetric	Concentric compressive	Transverse reinforcement
Kang et al. [25]	Solid rectangular columns	Plasticity	Discrete	Monotonic horizontal with axial force	Transverse reinforcement
Liu and Foster [26]	Solid rectangular columns	Microplane	Discrete	Concentric compressive	Transverse reinforcement
Barros [27]	Solid circular columns	Plasticity	Smeared axisymmetric	Concentric compressive	Transverse reinforcement
Imran and Pantazopoulou [28]	Solid circular columns	Plasticity	Smeared axisymmetric	Concentric compressive	Transverse reinforcement
Montoya et al. [29]	Solid rectangular columns	Nonlinear elasticity (MCFT)	Smeared (longitudinal) Discrete (transverse)	Concentric compressive	Transverse reinforcement
Attarnejad and Amirebrahimi [30]	Solid rectangular columns	Plasticity	Discrete	Concentric compressive	Transverse reinforcement
Johansson and Åkesson [31]	Solid circular columns	Plasticity	Smeared axisymmetric	Concentric compressive	Steel tube
Kwon and Spacone [32]	Solid rectangular columns	Nonlinear elasticity	Discrete	Monotonic horizontal with axial force	Transverse reinforcement
Hu et al. [33]	Solid circular columns	Plasticity	Smeared axisymmetric	Concentric compressive	Steel tube
Faria et al. [21]	Hollow rectangular piers in plane (2D)	Damage	Discrete	Cyclic horizontal with axial force	Transverse reinforcement
Luccioni and Rougier [34]	Solid circular columns	Damage - Plasticity	Smeared axisymmetric	Concentric compressive	Steel tube
Grassl and Jirásek [35]	Solid rectangular columns	Damage - Plasticity	Discrete	Eccentric compressive	Transverse reinforcement
Zergua and Naimi [36]	Solid rectangular and circular columns	Fracture - Plasticity	Discrete	Concentric compressive	Transverse reinforcement

2. Modelling framework and preliminary applications

The computational platform selected for the present study is a general finite element software (ATENA [37]), which satisfies the following essential criteria : (a) solid and linear finite element formulations for concrete and reinforcement, respectively, (b) reinforcement modelling with discrete or, preferably, embedded form, (c) robust nonlinear solvers capable to derive softening response and (d) friendly environment for pre-processing complex geometries and post-processing large amounts of output data. However, efficient modelling of concrete material behaviour under triaxial (confined) stress state required specific enhancements in the standard featured constitutive law. For this reason, an improved confinement-sensitive plasticity constitutive model for concrete in triaxial compression was developed, aiming to describe the strength and ductility enhancement of both normal and high-strength concrete under multiaxial compression [38]. This law included a three-parameter loading surface, uncoupled hardening and softening functions following the accumulation of plastic volumetric strain, and a nonlinear Lode-angle dependent plastic potential function. The various model parameters were calibrated on the basis of a large experimental database and were expressed in terms of uniaxial compressive concrete strength, practically leading to a single-parameter model. Further development was conducted for combining the above compressive constitutive law with a fracture model, based on the classical orthotropic smeared crack formulation and the crack band approach, in order to handle concrete cracking as well. The resulting fracture-plastic model [39] was incorporated in the aforementioned finite element software and its performance was evaluated by comparisons with various experimental results from the literature. As far as the steel constitutive law is concerned, a simple multilinear uniaxial law was utilised (Fig. 2).

The suggested modelling procedure [40] uses a fine mesh of 8-noded solid isoparametric elements for concrete and 2-noded truss elements for longitudinal and transverse reinforcement bars, which are embedded in the concrete solids. A major advantage of the present embedded formulation is that due to the independent node topology between solid (concrete) and linear (steel) element nodes, no modelling restrictions are imposed with respect to the complexity of the transverse reinforcement configuration (e.g. diagonal bars). When double symmetry is present, one quarter of the

section was modelled (using appropriate boundary conditions on symmetry planes) in order to reduce the computational cost and provide numerical stability. Since the numerical results have to reflect only the effect of transverse steel on concrete lateral expansion, horizontal nodal degrees of freedom on top and bottom planes were unrestrained (free) in order to capture the behaviour of an arbitrary block along the height of the vertical member, isolated from any local boundary conditions (e.g. connection to the foundation, deck, etc.). Concentric compressive loading was applied using prescribed displacements combined with a modified Newton-Raphson iterative scheme in order to retrieve a convergent solution beyond the attainment of section ultimate compressive strength (softening branch on the capacity curve) and hence determine the section deformation capacity as well. Figure 3 shows an overview of the aforementioned modelling techniques.

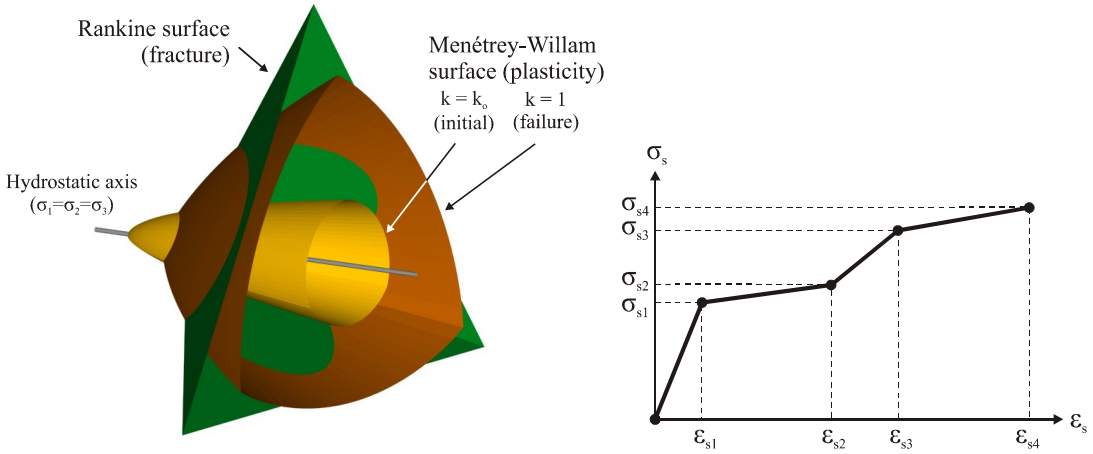

Figure 2. Constitutive laws for concrete (fracture-plastic, left) and steel (multilinear, right).

After analysis is performed, a capacity curve in terms of total axial reaction versus axial strain (R-ε) is retrieved. On this capacity curve, various performance and economic indices can be defined. Four confinement effectiveness indices are suggested herein, based on: (a) ultimate strength (K_R), (b) strain corresponding to ultimate strength (K_ε), (c) ductility based on strains ($K_{\varepsilon 85}$) and (d) ductility based on energy (K_{W85}). The ultimate axial strain is assumed equal to the strain corresponding to 85 % of the maximum axial reaction attained. Moreover, corresponding economic indices are derived (C_R, C_ε, $C_{\varepsilon 85}$ and C_{W85} respectively), equal to the above performance indices normalized by the transverse reinforcement volumetric ratio

($\rho_w = V_{transvese\ steel} / V_{confined\ concrete}$), which is an indirect measure of the steel material cost. All the above indices are defined with respect to a similar model containing only longitudinal reinforcement (i.e. unconfined). A detailed description of all the above indices is given in Figure 4.

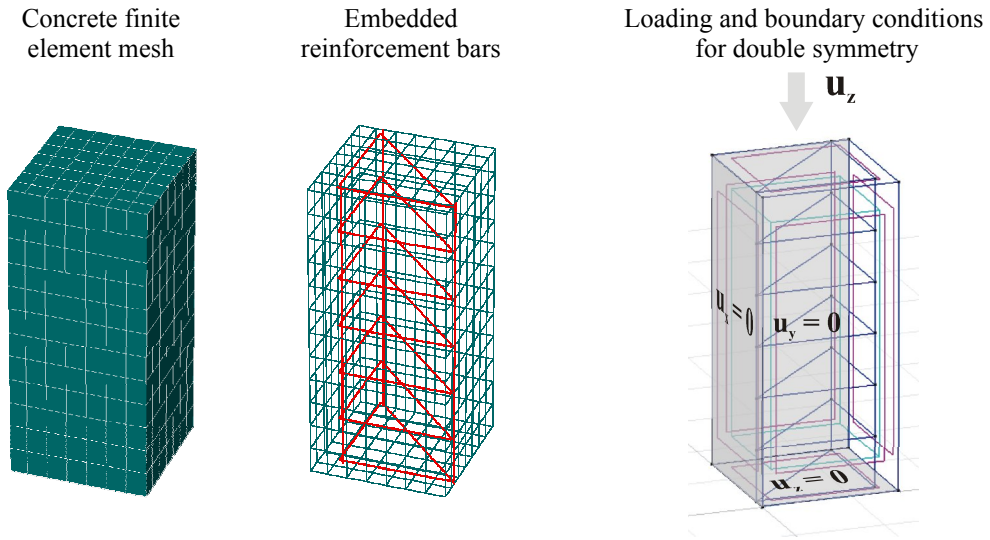

Figure 3. Concrete and reinforcement modelling, boundary conditions and loading.

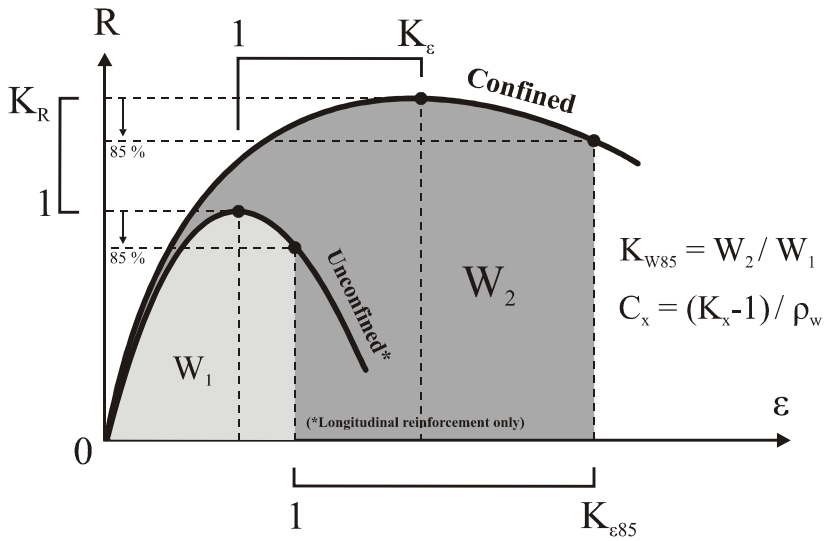

Figure 4. Definition of performance and economic indices.

An alternative method to estimate confinement effectiveness with respect to stress (similar to K_R) is herein introduced as *optical integration*, which performs stress averaging by scanning the coloured iso-areas produced by the finite element software

graphical postprocessor. The requested average value is calculated by the following simple expression :

$$\bar{\sigma} = \frac{\sum_{i=1}^{n} (\sigma_i \cdot p_i)}{n \cdot \sum_{i=1}^{n} p_i} \qquad (1)$$

where :

$\bar{\sigma}$ requested stress average value of the confined area

σ_i stress value corresponding to colour i

p_i total number of picture elements (pixels) corresponding to colour i

n total number of colours used

With the above procedure it is possible to accurately extract the average stress value over a part of a horizontal section cut, corresponding to the effectively confined region. The confinement effectiveness is then defined as $K_{OI} = \bar{\sigma} / f_c$. It was verified that using a total number of at least 20 colours, optical integration coincides with its typical numerical counterpart (node stress – times - node tributary area), though at a fraction of processing time. A similar concept applied elsewhere can be found in [41]. An important advantage is that this method can ignore the contribution of the concrete cover, which will be discussed later.

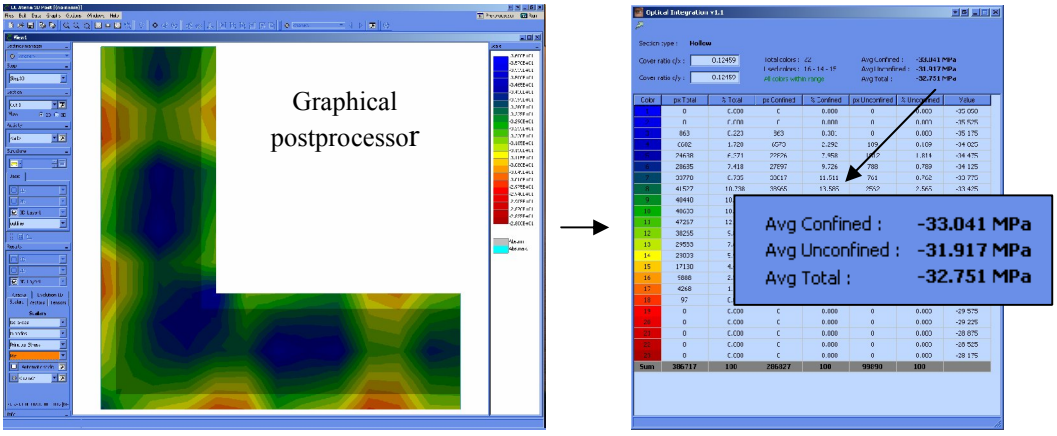

Figure 5. Application of the optical integration method.

A preliminary application of the suggested modelling procedure to reinforced concrete square columns of solid section is presented in the following. Three models were developed for experimental specimens tested by Sheikh and Uzumeri [6]. Apart from the originally tested models, downgraded versions in terms of reinforcement were also analysed, for comparison purposes (Fig. 6).

Model	Original	Downgraded (D)	Longitudinal only	Plain concrete
2A1-1 (Fig. 3) 305 x 305 mm s = 57.1 mm f_c = 31.88 MPa	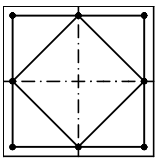	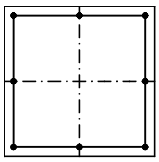	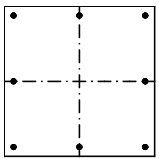	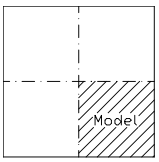
4B3-19 305 x 305 mm s = 101.6 mm f_c = 28.39 MPa	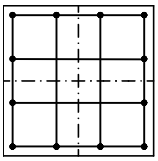	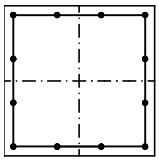	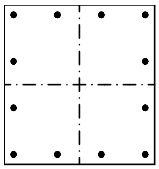	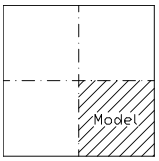
4D6-24 305 x 305 mm s = 38.1 mm f_c = 30.52 MPa	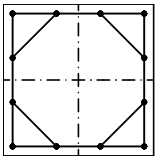	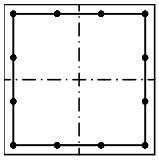	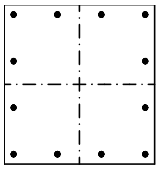	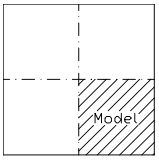

Figure 6. Square solid columns considered in the preliminary study.

Figure 7 shows a comparison between numerically and experimentally derived capacity curves for the three columns considered. It is observed that correlation is good in terms of deformation capacity with a small overestimation in terms of strength. This may be attributed to the possible early spalling of concrete cover (loss of material), longitudinal steel local buckling, boundary effects and accuracy of measurement devices during the experimental procedure. In the same figure, the axial compressive stress distribution on the element section is shown, where the effectively confined and unconfined regions are easily distinguished. Moreover, the cracking pattern at ultimate strain reasonably shows a concentration of splitting cracks across the column concrete cover.

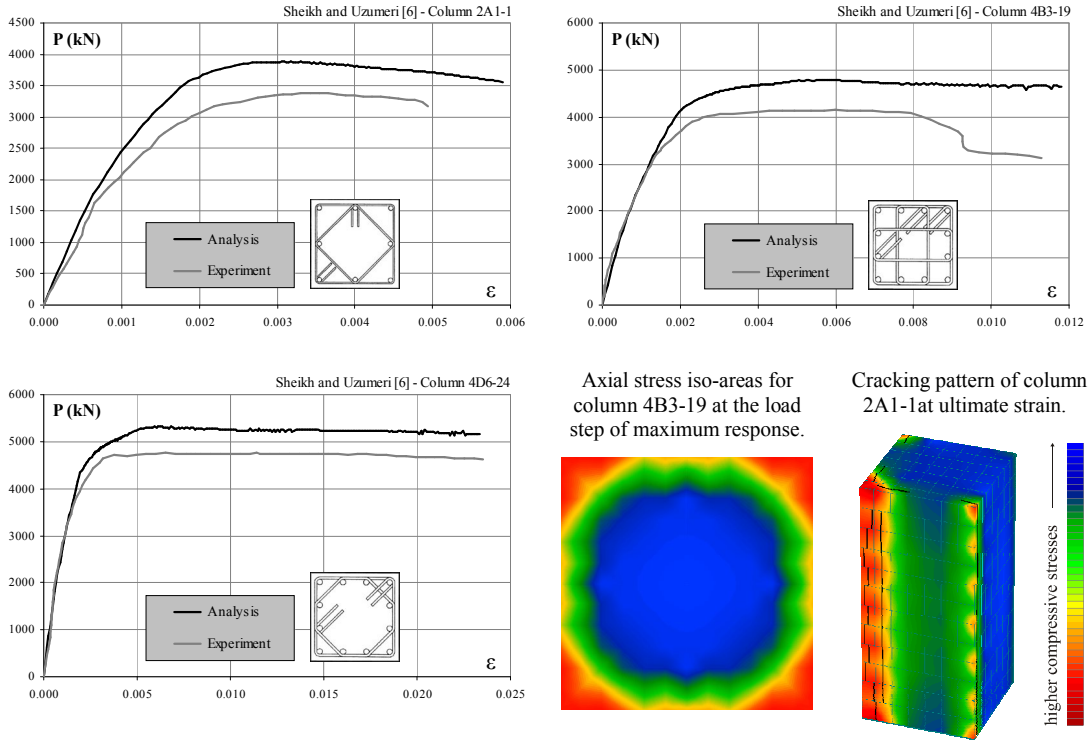

Figure 7. Capacity curves and graphical results from the square solid columns analysed.

The performance of the enhanced concrete constitutive law developed for the present study [39] is validated by comparing different reinforcement arrangements for the same column model. It is observed that, qualitatively, the expected strength and deformation increase for increasing complexity of transverse reinforcement arrangements is properly captured (Fig. 8). A quantitative comparison between confinement effectiveness in terms of strength between analysis and empirical models [10, 42] is presented in table 2. It is observed that the method of optical integration, which is focused only on the confined region of the section, shows very good correlation with empirical models. However, the derivation of confinement effectiveness based on capacity curves (K_R = $R_{confined}$ / $R_{unconfined}$) leads to an underestimation - yet consistent - of the respective empirical values, which is mainly attributed to the inclusion of the unconfined concrete in the capacity curve. Pending a more extensive verification, it can be concluded that the suggested methodology can sufficiently simulate the expected structural behaviour of confined vertical members and hence is eligible for application in a broad range of solid and hollow bridge pier models, which will be described in the subsequent section.

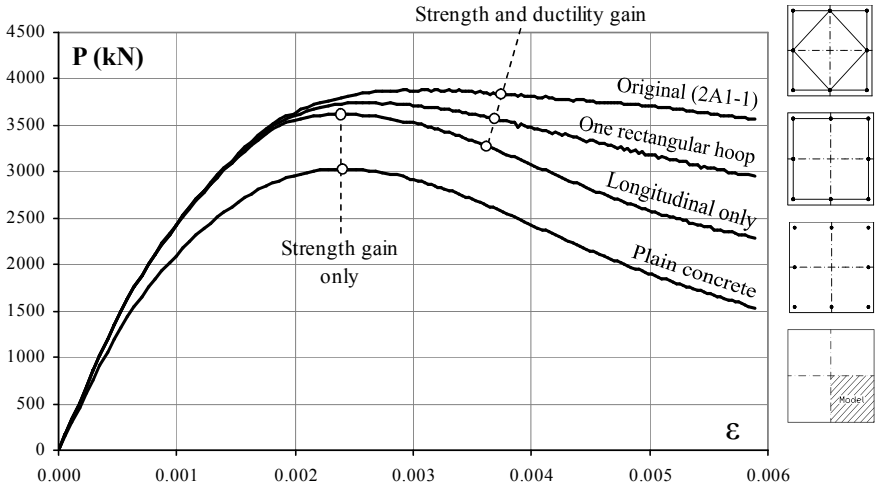

Figure 8. Strength and ductility enhancement due to confinement for column 2A1-1.

Table 2. Comparison of strength enhancement between present analysis and empirical models

Column model	From capacity curves	From optical integration	ρ_w	From Park et al. [10] : $K = 1 + \rho_w \cdot \frac{f_{yw}}{f_c}$	From Kappos [42] : $K = 1 + a \cdot \left(\rho_w \cdot \frac{f_{yw}}{f_c} \right)^b$		
	K_R	K_{OI}	%	K	a	b	K
2A1-1	1.07	1.13	0.80	1.14	1.0	1.0	1.14
2A1-1(D)	1.03	1.07	0.47	1.08	0.55	0.55	1.08
4B3-19	1.20	1.40	1.70	1.29	1.25	1.0	1.36
4B3-19(D)	1.05	1.10	0.73	1.12	0.55	0.75	1.11
4D6-24	1.28	1.55	2.25	1.35	1.0	1.0	1.35
4D6-24(D)	1.09	1.14	1.25	1.20	0.55	0.75	1.16

3. Bridge pier models

The bridge pier models considered in this study were based on actually constructed bridges across the Egnatia highway in northern Greece. The main pier types modelled were circular solid, circular hollow (2 different types), rectangular solid (wall-type) and rectangular hollow (3 different types) (Fig. 9).

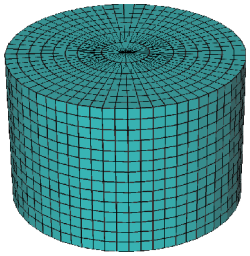

Circular solid sections (CSS) :

Diameter 1.50 m
Concrete cover 5 cm

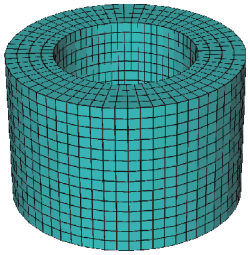

Circular hollow sections (CHS) :

Outer diameter 1.50 m

Type 1 (CHS1) : Thickness 30 cm
Type 2 (CHS2) : Thickness 45 cm

Concrete cover 5 cm

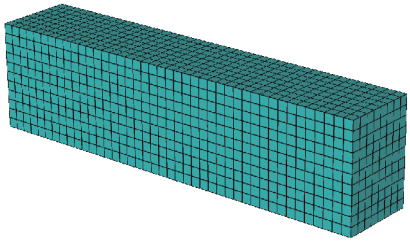

Rectangular solid sections (RSS), ¼ shown :

Dimensions 7.80 × 1.50 m
Sparse and dense arrangements
Concrete cover 5 cm

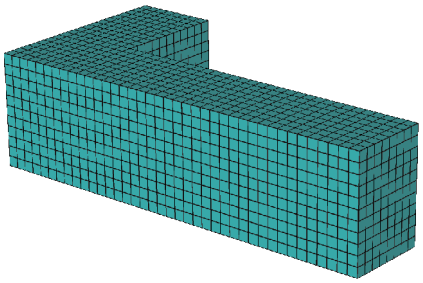

Rectangular hollow sections (RHS), ¼ shown :

Type 1 (RHS1) : 7.80 × 1.50 m, thickness 74 cm
Sparse and dense arrangements
Type 2 (RHS2) : 4.00 × 4.00 m, thickness 40 cm
Type 3 (RHS3) : 5.50 × 2.75 m, thickness 30 cm

Concrete cover 5 cm

Figure 9. Concrete solid element meshes for pier section types considered.

The section height of all models was set equal to z = 1.0 m and the finite element mesh was designed towards : (a) a solid element aspect ratio near unity and (b) the finest possible density, yet bound by an upper limit of about 5000 ~ 6000 solid elements, beyond which the computational cost and volume of results were excessive. A preliminary analysis confirmed that numerical results were practically insensitive to both section height and finite element mesh density (Fig. 10).

The transverse reinforcement arrangements (grade S500s) that was embedded to the above solid element meshes included (a) spiral or hoop circular reinforcement, with or without transverse links for circular sections (Fig. 11) and (b) transverse links, overlapping hoops or a combination of transverse links with diagonal links [17] for

rectangular sections (Fig. 12). The overlapping hoop arrangements were designed so as to coincide with their transverse link counterparts, having the lowest possible aspect ratio (square-like). For achieving this, additional transverse links were added to the reinforcement pattern, only when necessary (see Figure 12). Other parameters, also considered, were the transverse reinforcement spacing (10, 15 or 20 cm), the horizontal arrangement density (sparse and dense, corresponding to the pier mid-height and base respectively, for rectangular sections RSS and RHS1) and concrete strength (normal : C20/25 and high : C50/60). The present parametric analysis included a total of 183 different models (detailed model drawings and tables can be found in [43]), the total solution time exceeded 300 hours (running 2 analyses simultaneously) and the total size of results reached 2 terabytes.

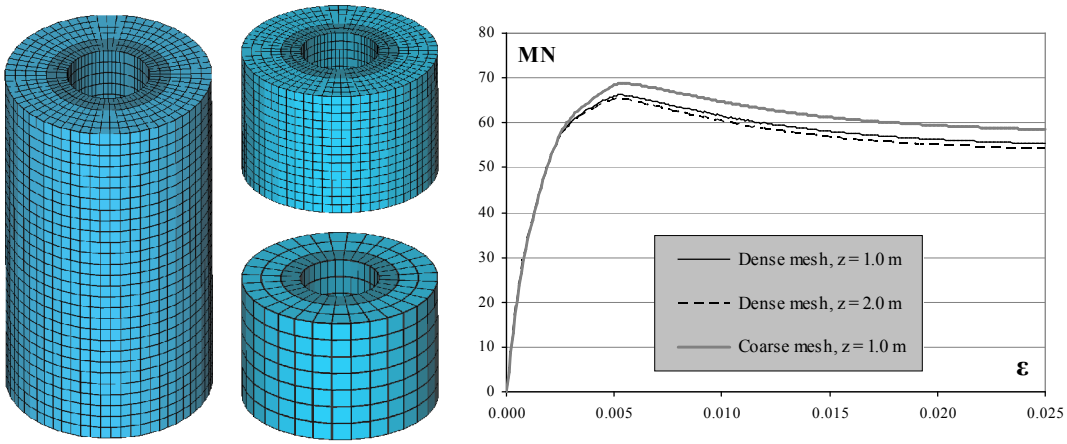

Figure 10. Capacity curve comparison for different heights and mesh densities.

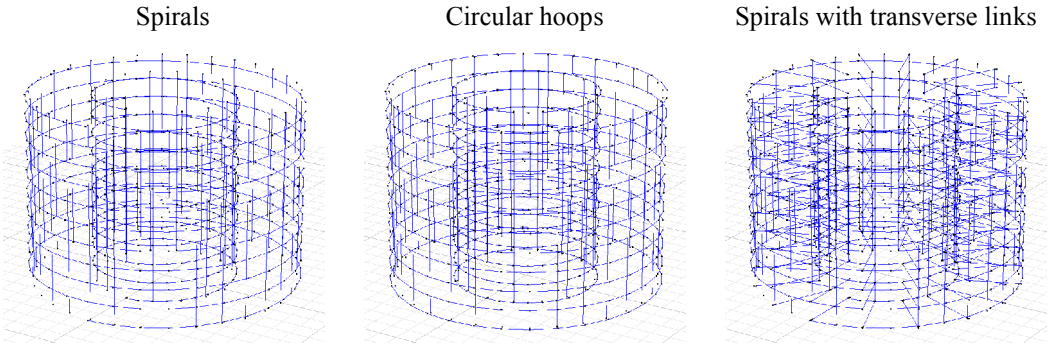

Figure 11. Various transverse reinforcement arrangements for circular sections.

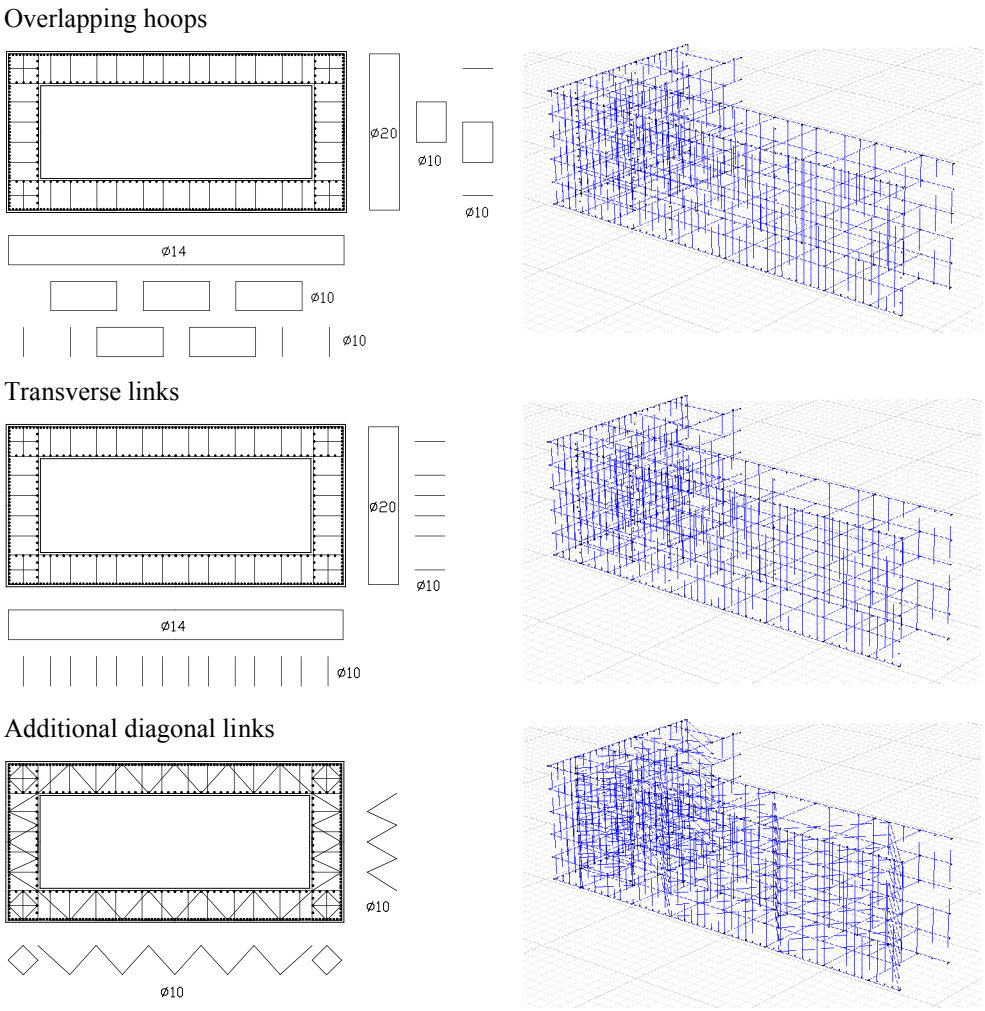

Figure 12. Various transverse reinforcement arrangements for rectangular sections.

4. Further modelling considerations

In this section, various modelling assumptions adopted in the suggested methodology are discussed in detail, to determine their effect on the present analysis results. These assumptions, namely (a) ignoring local buckling in the longitudinal reinforcement, (b) ignoring the flexural stiffness of transverse reinforcement, (c) ignoring the effect of cover spalling and (d) ignoring geometric nonlinearity (second order effects), are also adopted in the majority of similar studies on the issue of confinement (e.g. [22, 29, 32] amongst others), wherein a discussion of the implications of these assumptions is lacking.

4.1 Effect of longitudinal reinforcement buckling

It is well known that a favourable effect of closely spaced transverse reinforcement is that early buckling of the longitudinal reinforcement is prevented [5]. In the pier models described in the previous section, the possibility of longitudinal reinforcement buckling was ignored, even where hoop spacing was relatively wide (more than about 5 times the longitudinal bar diameter); the implications of this assumption will be investigated here.

For concentrically compressed elements like longitudinal reinforcement bars, the expected failure mode is inelastic buckling which follows yielding and is attributed to substantial reduction in the secant stiffness of steel [5].

The effect of inelastic buckling is a rather complex issue and has been studied both experimentally and analytically in the past (e.g. [44, 45, 46]). For the present evaluation, the empirical expressions by Yalcin and Saatcioglu [45] have been selected for their simplicity, defining a downscaled stress-strain law for steel in compression, in order to account for the effect of inelastic buckling. For s/D < 4.5 (or < 5.0 according to [44]) the steel response in compression coincides with that in tension (unaltered), for $4.5 \leq s/D \leq 8.0$ hardening becomes milder and for the extreme case of s/D > 8, steel yielding is followed by material softening. For the latter case, the control point (f_u , ε_u) for defining the softening branch is :

$$f_u = 28 \cdot \left(\frac{s}{D}\right)^{-1.7} \cdot f_y \tag{1}$$

$$\varepsilon_u = \left[40 - 6 \cdot \ln\left(\frac{s}{D}\right)\right] \cdot \varepsilon_y \tag{2}$$

From the above definition, it is possible to include the inelastic buckling effect in the finite element analysis, by appropriate modification in the steel stress-strain law. In Figure 13, the modified stress strain law and a comparison between capacity curves with and without the effect of inelastic buckling is shown for model RHS2-12 (rectangular hollow pier, 4.00 × 4.00 m, thickness 40 cm, s = 20 cm, D = 16 mm, s/D = 12.50), representing an extreme case within the model's applicability range described in the previous paragraph. It is observed that the difference in model response is negligible

and hence it is generally concluded that ignoring the effect of longitudinal reinforcement buckling does not practically affect the validity of the present analysis results.

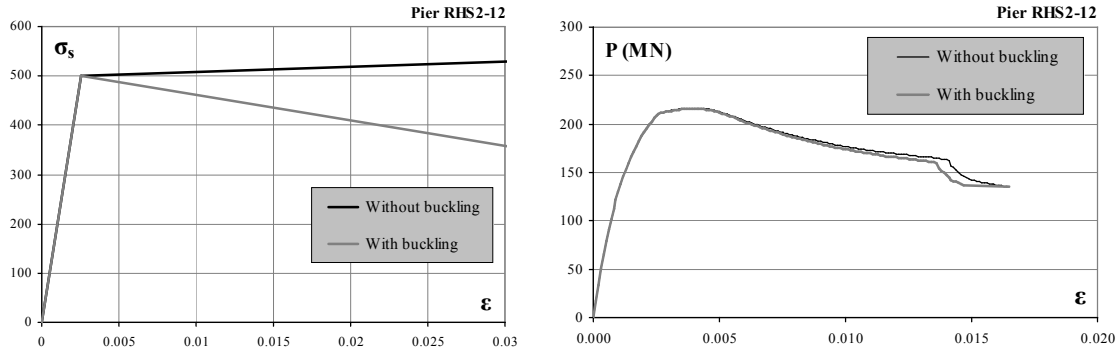

Figure 13. Modified steel law to account for inelastic buckling (left) and comparison between capacity curves including and excluding inelastic buckling effect (right).

4.2 Effect of transverse reinforcement flexural stiffness

In this section it is investigated whether the customary assumption of modelling reinforcement bars using truss elements is adequate for the present analysis. Truss elements are characterized by axial stiffness across the element length and zero flexural stiffness in the normal direction. It is well known that during axial compression of a reinforced concrete vertical member, the transverse reinforcement is activated and restrains the physical lateral expansion of concrete (passive confinement). After yielding of transverse reinforcement bars, their reaction forces remain almost constant (further increase due to hardening is small), resulting to active confinement conditions. The critical question is the physical mechanism of load transmission from steel bars to the concrete confined core. Answers provided in previous studies are rather contradictory. Saatcioglu and Ravzi [47] and Yalcin and Saatcioglu [45] assumed that confinement forces can be modelled by a varying pressure distribution, constituting of point forces due to the axial rigidity of transverse reinforcement and distributed forces due to their flexural rigidity. However, for the sake of simplicity, the above varying distribution is ultimately converted to an *equivalent uniform confinement pressure* based on empirical factors (Fig. 14). Although this assumption may be valid for circular

sections, where the ring tension of the transverse reinforcement can be efficiently replaced by a uniform radial pressure towards the section centre [5], in rectangular sections it can lead to a serious overestimation of the actual contribution of transverse reinforcement, especially for sparsely spaced bars in plan [47]. Another fact that favours the above statement is that the flexural stiffness of a reinforcement bar (EI) is practically negligible compared to its axial stiffness (EA, e.g. EA/EI = 81,600 for D = 14 mm and EA/EI = 250,000 for D = 8 mm), and hence the aforementioned equivalent uniform confinement pressure considerably favours the (negligible) flexural stiffness of reinforcement bars against their (significant) axial counterpart.

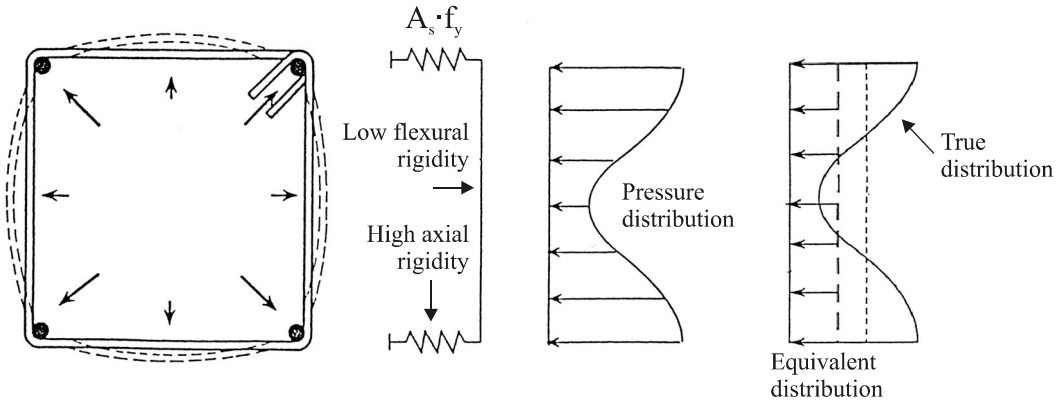

Figure 14. Lateral force distribution due to confinement according to Yalcin and Saatcioglu [45].

In order to determine the effect of the flexural rigidity of transverse reinforcement on the stress distribution in the concrete core and hence on the confinement effectiveness, a parametric analysis was performed. Since beam elements for reinforcement modelling were not available in the finite element software (ATENA) used, the analysis was performed using the SAP2000 software [48]. Specifically, a square concrete section of 20 × 20 cm was modelled in plane using elastic concrete material (E_c = 29 GPa, ν = 0.2) assigned to 1600 shell finite elements. Beam linear elements were attached in the perimeter of the section, using steel material (E_s = 200 GPa) and circular section of D = 10 mm. Lateral expansion of concrete was simulated implicitly by a thermal loading of +1 ^{o}C and by assigning a temperature factor of $\alpha = 2.5 \cdot 10^{-3}$ to the concrete material, so that a transverse strain equivalent to steel yielding (f_{yw} / E_c = 2.5 ‰) will develop. The analysis was elastic with the assumption of small strains. For comparison reasons, the above procedure was repeated for modified steel material properties in terms of flexural

rigidity (zero for modelling truss action, multiples of 10, 100, 1000 and infinite for laterally rigid action). Figure 15 shows a comparison between different models of the above parametric analysis in terms of in-plane stress ($\sigma_1 = \sigma_2$) and reinforcement flexural moments. It is clearly observed that the actual effect of the flexural rigidity of reinforcement bars is negligible and may become significant for a fictitious (and unrealistic) multiplier of at least 100. Moreover, it is shown that a constant stress state inside the concrete core (which corresponds to the aforementioned empirical assumption of equivalent uniform confinement pressure) can be achieved only by using infinite flexural rigidity on the beam elements, which is totally unrealistic.

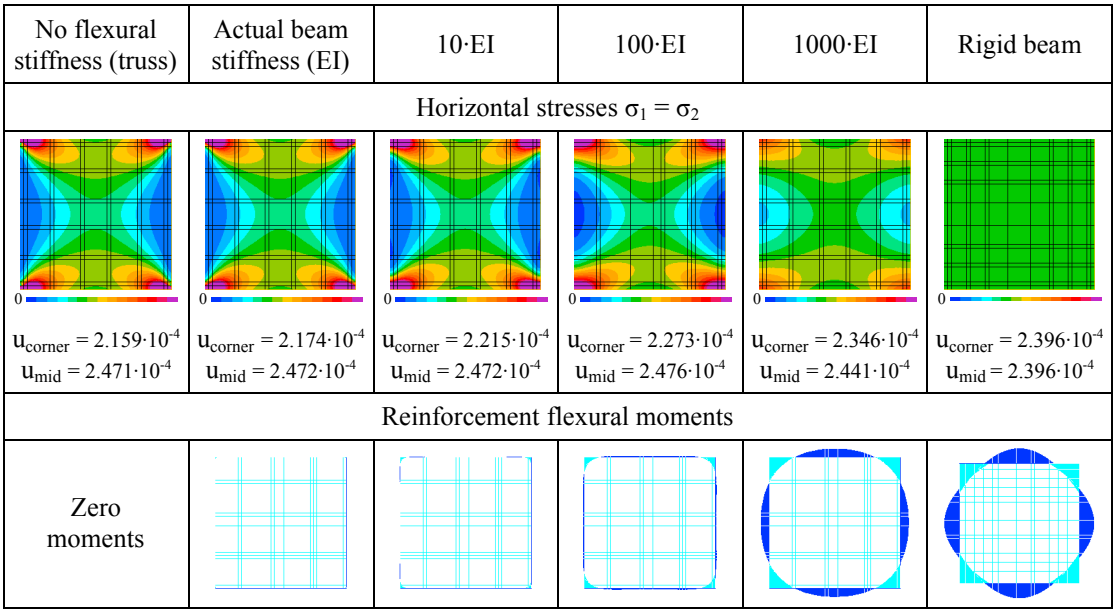

Figure 15. Parametric investigation on the effect of flexural rigidity of reinforcement bars.

The opposite assumption of the exclusively axial contribution of reinforcement bars, which is compatible with truss element modelling, has been investigated analytically by Karabinis and Kiousis [49], where transverse reinforcement actions were simulated using external point forces (Fig. 16). For validating the above assumption, additional analysis has been performed using two different 3D square column models of 20 × 20 cm section (a) using truss elements for confinement reinforcement and (b) using external nonlinear springs applied on the four column corners, having the same uniaxial stress-strain law for steel (Fig. 17). The hoop diameter was set to 8 mm and loading was axial compressive prescribed displacement. Figure 18 shows a comparison between the ensuing capacity curves for the two modelling procedures. It is observed that

differences are relatively small (3.4 % in terms of ultimate strength and 12 % in terms of corresponding strain) and that modelling with truss elements shows slightly increased confinement effectiveness, which is attributed to the continuous axial contribution of truss elements across the column edges instead of only point reactions in the corners. Consequently, from the above discussion, it is generally concluded that the use of truss elements in the present analytical study is clearly adequate for confinement modelling.

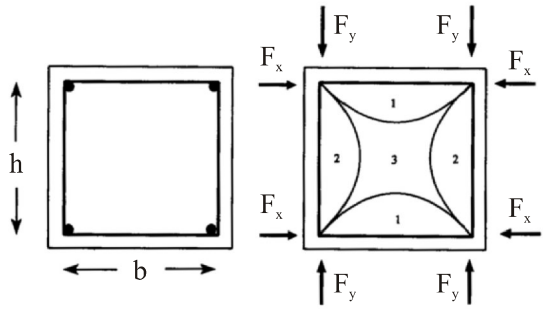

Figure 16. Lateral force distribution due to confinement according to Karabinis and Kiousis [49].

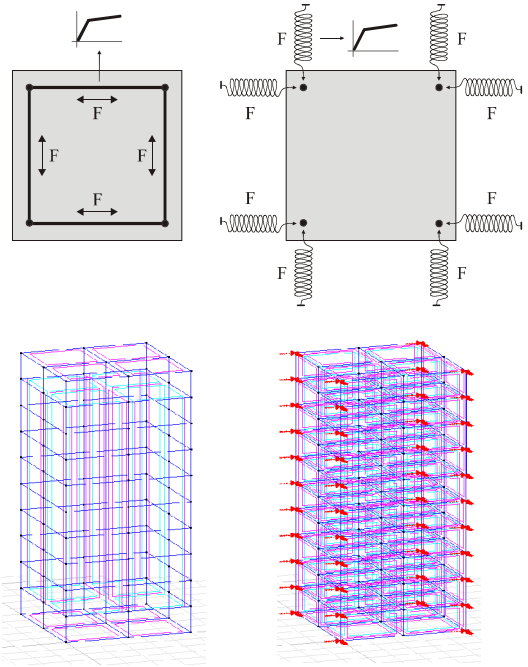

Figure 17. Modelling confinement with truss elements and nonlinear springs.

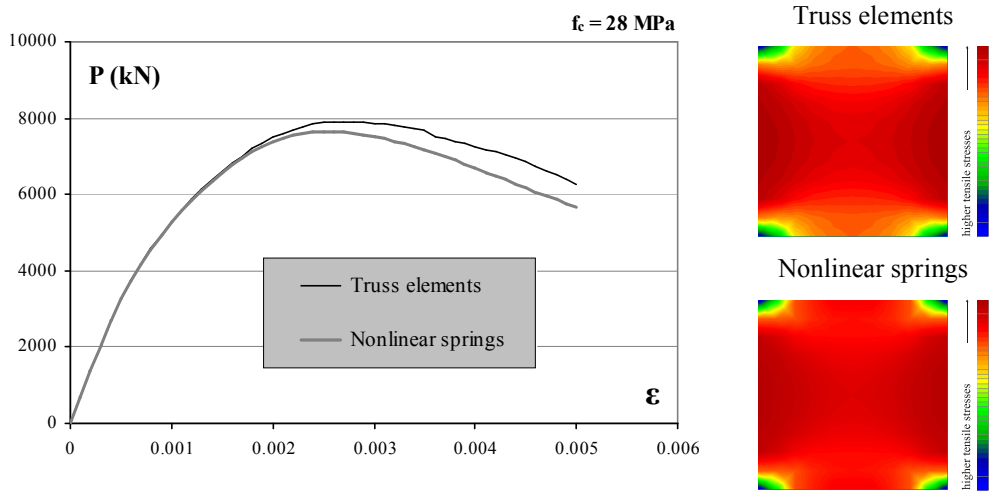

Figure 18. Comparison between capacity curves and in-plane stress distribution (at ultimate strength) between truss elements and nonlinear springs for confinement modelling.

4.3 Effect of cover spalling

It has been experimentally observed (e.g. [6, 9]) that for reinforced concrete vertical members under axial compressive loading, the unconfined concrete cover tends to spall off from the confined concrete core, even for low levels of axial strain. This effect can be attributed to the high tensile strains that develop on the cover-core interface due to Poisson's effect and the presence of transverse reinforcement [24]. Although cover concrete cracking is successfully captured by the present analysis (Fig. 7), cracked material can still sustain compressive stresses, since it is not physically removed from the finite element model as the actual phenomenon implies. This issue has been previously handled numerically by Liu and Foster [26] by automatically assigning zero stiffness to cover finite elements when the transverse cover-core interface strain exceeds an empirically defined threshold value. However, this feature was not supported by the software used herein (nor by most other packages available), therefore analysis was performed assuming no cover spalling.

A direct effect of the above limitation was the small overestimation of the ultimate strength of columns studied in the preliminary analysis compared to experimental results (Fig. 7). In order to further investigate the issue, column 2A1-1 [6] was solved again without modelling the concrete cover, as suggested in [28]. It is observed that the

experimental response lies between the two approaches (with and without cover), which is justified by the fact that cover spalling is usually partial, as depicted in the experimental failure mode (Fig. 19-left).

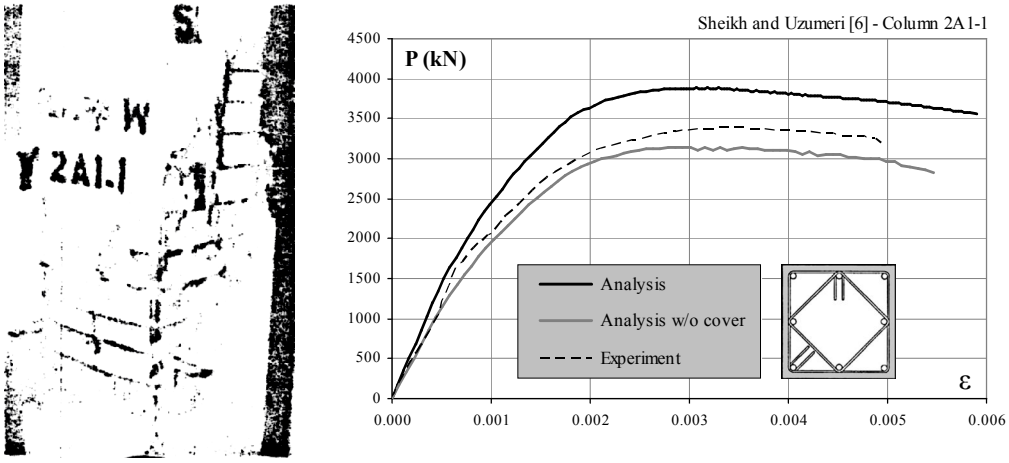

Figure 19. Cover spalling for column 2A1-1 (left, [6]) and capacity curves for analysis with and without concrete cover (right).

Since the assumption of ignoring cover spalling is retained throughout the present study, it is deemed that it cannot affect the *comparative* assessment of confinement effectiveness among different transverse reinforcement configurations on the same model geometry. It is also noted that the method of optical integration is not affected by the presence or absence of concrete cover. Specifically, for the above column (Fig. 19), the derived effectiveness in terms of strength (K_{OI}), when cover is included, is equal to 1.13 (Tab. 2) and equal to 1.14 otherwise Nevertheless, the evaluation of confinement effectiveness based on capacity curves will be preferred in this study because it also provides insight in terms of ductility, especially based on energy (K_{W85}). It has been already noted that the latter method underestimates the effectiveness provided by optical integration (based on strength), but this is done in a consistent manner (Fig. 20) and hence it cannot possibly affect the evaluation procedure.

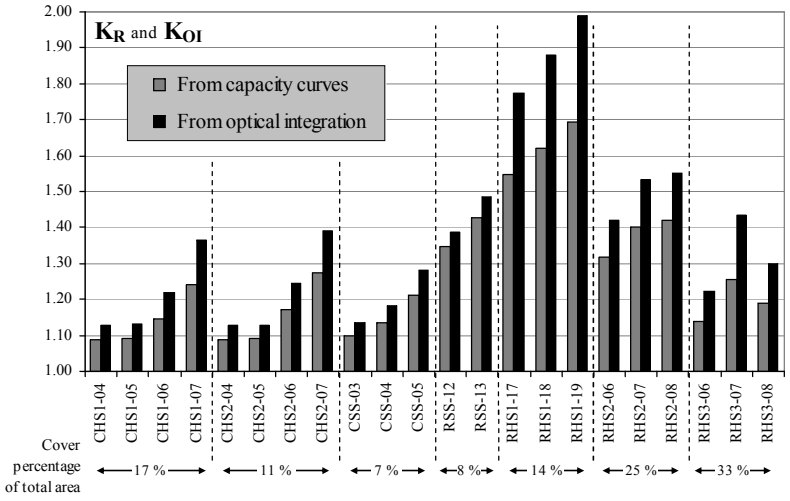

Figure 20. Comparison of confinement effectiveness indices in terms of strength between capacity curves (K_R) and optical integration (K_{OI}) for various pier models considered in the present study.

4.4 Effect of geometric nonlinearity

In the present analysis, small displacements were assumed, i.e. equilibrium is imposed on the undeformed shape during the nonlinear solution [22]. To investigate the validity of this assumption, a few pier models were re-analysed by enabling geometric nonlinearity in the finite element solver. From comparative plots shown in Figure 21, it is observed that there are negligible differences between the two alternative methods. It is noted though, that for model RHS1-17, where brittle failure in post-peak is observed (will be discussed in detail in the companion paper), geometric nonlinearity seems to slightly expedite this failure mode. Nonetheless, considering the substantial increase in the computational cost for enabling second-order effects, the use of small displacements is a one-way solution in the context of the present study.

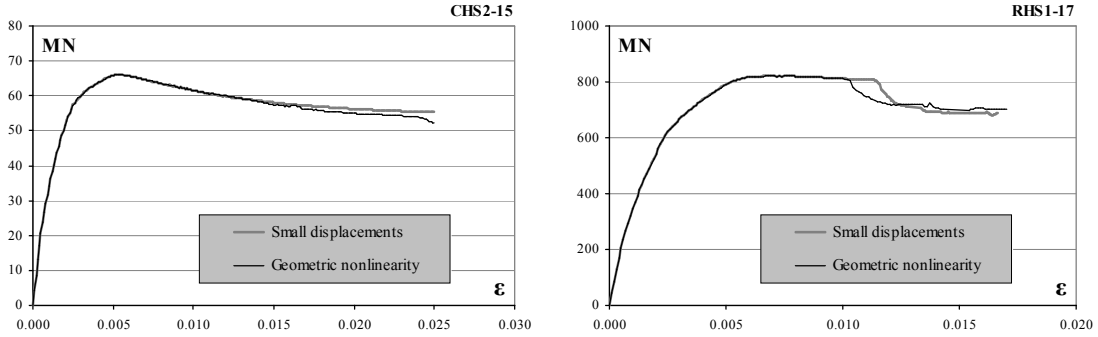

Figure 21. Comparison between capacity curves using small displacements and geometric nonlinearity.

5. Conclusions

In this paper, a consistent methodology for modelling both solid and hollow reinforced concrete bridge pier sections with various transverse reinforcement arrangements was suggested, using a general-purpose finite element software. The issues covered were the constitutive laws used, finite element modelling, post-processing methods, and a discussion on various issues related to the numerical simulation of confinement effects. It can be generally concluded that three-dimensional analysis can be established as a promising alternative to empirical confinement models because it is unrestricted in terms of section geometry and reinforcement arrangement complexities. It can be also considered as a cost-effective counterpart to experimental testing towards the assessment and design of (especially hollow) reinforced concrete bridge piers.

The ultimate objective of the present research is to suggest the most effective and convenient confinement arrangements in terms of enhanced strength and ductility, as well as ease of construction and cost effectiveness, on the basis of a broad parametric analysis including circular and rectangular bridge piers of solid and hollow section, based on actually constructed bridges. This issue will be covered in a companion paper including the interpretation and evaluation of the respective numerical results.

Acknowledgement

This work has been performed within the framework of the research project 'ASProGe : Seismic Protection of Bridges', funded by the General Secretariat of Research and Technology (GGET) of Greece.

References

[1] Eurocode 8. Design of Structures for Earthquake Resistance. European Committee for Standardization, 2005.
[2] American Association of State Highway and Transportation Officials (AASHTO). LRFD Bridge Design Specifications. Washington D.C., USA, 2004.
[3] Priestley, M.J.N. Seismic design issues for hollow bridge piers. Report No. 98/01, Egnatia Odos S.A., Greece, September 1998.
[4] *fib* Seismic design and retrofit – structural solutions. Bulletin No. 39; 300 pp.
[5] Penelis, G.G., Kappos, A.J. Earthquake resistant concrete structures. E & FN SPON, Chapman & Hall, London, 1997.
[6] Sheikh, S.A., Uzumeri, S.M. Strength and ductility of tied concrete columns. Journal of the Structural Division, ASCE 1980;108(4):929-50.
[7] Scott, B.D., Park, R., Priestley, M.J.N. Stress-strain behavior of concrete confined by overlapping hoops at low and high strain rates. ACI Journal 1982;79(1):13-27.
[8] Yong, Y.K., Nour, M.G., Nawy, E.G. Behavior of laterally confined high-strength concrete under axial loads. Journal of Structural Engineering, ASCE 1988;114(2):332-51.
[9] Ravzi, S.R., Saatcioglu, M. Tests of high strength concrete columns under concentric loading. Report OCEERC 96-03, Department of Civil Engineering, University of Ottawa, Canada.
[10] Park, R., Priestley, M.J.N., Gill, W.D. Ductility of square confined concrete columns. Journal of the Structural Division, ASCE 1982;108(4):929-50.
[11] Sheikh, S.A., Uzumeri, S.M. Analytical model for concrete confinement in tied columns. Journal of the Structural Division, ASCE 1982;108(12):2703-22.
[12] Mander, J.B., Priestley, M.J.N., Park, R. Theoretical stress-strain model for confined concrete. Journal of the Structural Division, ASCE 1988;108(8):1804-26.
[13] Papanikolaou, V.K., Kappos, A.J. Constitutive model for concrete in triaxial compression and applications in finite element analysis of R/C bridge piers. 6th GRACM International Congress on Computational Mechanics, Thessaloniki, Greece, June 2008.
[14] Mander, J.B., Priestley, M.J.N., Park, R. Behavior of hollow reinforced concrete columns. Bulletin of New Zealand National Society for Earthquake Engineering 1983;16(4):273-90.
[15] Morkin, Z.A., Rumman, W.S. Ultimate capacity of reinforced concrete members of hollow circular sections subjected to monotonic and cyclic bending. ACI Structural Journal 1985;82(5):653-6.
[16] Yeh, Y.K., Mo, Y.L., Yang, C.Y. Seismic performance of hollow circular bridge piers. ACI Structural Journal 2001;98(6):862-71.
[17] Pinto, A.V. (Ed.) Pseudo-dynamic and shaking table tests on R/C bridges. ECOEST/PREC8 Report, No. 5.
[18] Taylor, A.W., Rowell, R.B., Breen, J.E. Behavior of thin-walled concrete box piers. ACI Structural Journal 1995;92(3):319-33.
[19] Mo, Y.L., Wong, D.C., Maekawa, K. Seismic performance of hollow bridge columns. ACI Structural Journal 2003;100(3):337-48.
[20] Sheikh, S.A. A comparative study of confinement models – Discussion by R. Park, A. Fafitis, S.P. Shah, and Author. ACI Journal 1982;80(3):260-5.
[21] Faria, R., Pouca, N.V., Delgado, R. Simulation of the cyclic behaviour of R/C rectangular hollow section bridge piers via a detailed numerical model. Journal of Earthquake Engineering 2004;8(5):725-48.

[22] Abdel-Halim, M.A.H., Abu-Lebdeh, T.M. Analytical study for concrete confinement in tied columns. Journal of Structural Engineering, ASCE 1989;115(11):2810-28.
[23] Barzegar, F., Maddipudi, S. Three dimensional modeling of concrete structures I : Plain concrete. Journal of Structural Engineering, ASCE 1997;123(10):1339-46.
[24] Foster, S.J., Liu, J., Sheikh, S.A. Cover spalling in HSC columns loaded in concentric compression. Journal of Structural Engineering, ASCE 1998;124(12):1431-7.
[25] Kang, H.D., Willam, K.J., Shing, B., Spacone, E. Failure analysis of R/C columns using a triaxial concrete model. Computers and Structures 2000;77(5):423-40.
[26] Liu, J., Foster, S.J. A three-dimensional finite element model for confined concrete structures. Computers and Structures 2000;77(5):441-51.
[27] Barros, M. Elasto-plastic modelling of confined concrete elements following MC90 equations. Engineering Structures 2001;23(4):311–8.
[28] Imran, I., Pantazopoulou, S.J. Plasticity model for concrete under triaxial compression. Journal of Engineering Mechanics, ASCE 2001;127(3):281-90.
[29] Montoya, E., Vecchio, F.J., Sheikh, S.A. Compression field modeling of confined concrete. Structural Engineering and Mechanics 2001;92(3):311-8.
[30] Attarnejad, R., Amirebrahimi, A.M. Load-displacement curves of square reinforced concrete columns based on fracture mechanics. Proceedings of the 15th ASCE Engineering Mechanics Conference, Columbia University, New York, June 2-5, 2002.
[31] Johansson, M., Åkesson, M. Finite element study on concrete-filled steel tubes using a new confinement sensitive concrete compression model. Nordic Concrete Research 2002;27:43-62.
[32] Kwon, M., Spacone, E. Three-dimensional analysis of reinforced concrete columns. Computers and Structures 2002;80(2):199-212.
[33] Hu, H.T., Huang, C.S., Wu, M.H., Wu, Y.M. Nonlinear analysis of axially loaded concrete-filled tube columns with confinement effect. Journal of Structural Engineering, ASCE 2003;129(10):1322-9.
[34] Luccioni, B.M., Rougier, V.C. A plastic damage approach for confined concrete. Computers and Structures 2005;83(27):2238-56.
[35] Grassl, P., Jirásek, M. Damage-plastic model for concrete failure. International Journal of Solids and Structures 2006;43(22-23):7166-96.
[36] Zergua, A., Naimi, M. Elastic-plastic fracture analysis of structural columns. Journal of Civil Engineering and Management 2006;12(2):181-7.
[37] Červenka, V., Jendele, L., Červenka, J. ATENA Program Documentation. Part 1 : Theory. Červenka Consulting, Prague, Czech Republic, 2008.
[38] Papanikolaou, V.K., Kappos, A.J. Confinement-sensitive plasticity constitutive model for concrete in triaxial compression. International Journal of Solids and Structures 2007;44(21):7021-48.
[39] Červenka, J., Papanikolaou, V.K. Three dimensional combined fracture-plastic material for concrete. International Journal of Plasticity 2008;24(12):2192-220.
[40] Papanikolaou, V.K., Kappos, A.J. Modelling confinement in concrete columns and bridge piers through 3D nonlinear finite element analysis. *fib* Symposium Keep Concrete Attractive, Budapest, Hungary, May 2005;488-95.
[41] Sfakianakis, M.G. Biaxial bending with axial force of reinforced, composite and repaired concrete sections of arbitrary shape by fiber model and computer graphics. Advances in Engineering Software 2002;33(4):227-42.
[42] Kappos, A.J. Analytical prediction of the collapse earthquake for R/C buildings : Suggested methodology. Earthquake Engineering and Structural Dynamics 1991;20(2):167-76.
[43] Papanikolaou, V.K. Analytical Study of Confined Reinforced Concrete Members using the Three-Dimensional Nonlinear Finite Element Method. PhD Thesis (in Greek), Civil Engineering Department, Aristotle University of Thessaloniki, Thessaloniki, Greece, 2007.
[44] Mau, S.T. Effect of tie spacing on inelastic buckling of reinforcing bars. ACI Structural Journal 1990;87(6):671-7.
[45] Yalcin, C., Saatcioglu, M. Inelastic analysis of reinforced concrete columns. Computers and Structures 2000;77(5):539-55.
[46] Bae, S., Mieses, A.M., Bayrak, O. Inelastic buckling of reinforcing bars. Journal of Structural Engineering, ASCE 2005;131(2):314-21.
[47] Saatcioglu, M., Ravzi, S.R. Strength and ductility of confined concrete. Journal of the Structural Division, ASCE 1992;118(6):1590-607.

[48] Computers and Structures SAP2000 – Linear and nonlinear static and dynamic analysis and design of three-dimensional structures. Computers and Structures Inc., Berkeley, California, USA, 2006.
[49] Karabinis, A.I., Kiousis, P.D. “Strength and ductility of rectangular concrete columns : A plasticity approach. Journal of Structural Engineering, ASCE 1996;122(3):267-74.